Localization of the *Bacillus subtilis murB* Gene within the *dcw* Cluster Is Important for Growth and Sporulation

Gonçalo Real and Adriano O. Henriques*

Instituto de Tecnologia Química e Biológica, Universidade Nova de Lisboa, Avenida da República, Apartado 127, 2781-901 Oeiras Codex, Portugal

The *Bacillus subtilis murB* gene, encoding UDP-*N*-acetylenolpyruvoylglucosamine reductase, a key enzyme in the peptidoglycan (PG) biosynthetic pathway, is embedded in the *dcw* (for "division and cell wall") cluster immediately upstream of *divIB*. Previous attempts to inactivate *murB* were unsuccessful, suggesting its essentiality. Here we show that the cell morphology, growth rate, and resistance to cell wall-active antibiotics of *murB* conditional mutants is a function of the expression level of *murB*. In one mutant, in which *murB* was insertionally inactivated in a merodiploid bearing a second xylose-inducible P*xylA-murB* allele, DivIB levels were reduced and a normal growth rate was achieved only if MurB levels were threefold that of the wild-type strain. However, expression of an extra copy of *divIB* restored normal growth at wild-type levels of MurB. In contrast, DivIB levels were normal in a second mutant containing an in-frame deletion of *murB* (Δ*murB*) in the presence of the P*xylA-murB* gene. Furthermore, this strain grew normally with wild-type levels of MurB. During sporulation, the levels of MurB were highest at the time of synthesis of the spore cortex PG. Interestingly, the Δ*murB* P*xylA-murB* mutant did not sporulate efficiently even at high concentrations of inducer. Since high levels of inducer did not interfere with sporulation of a *murB*⁺P*xylA-murB* strain, it appears that ectopic expression of *murB* fails to support efficient sporulation. These data suggest that coordinate expression of *divIB* and *murB* is important for growth and sporulation. The genetic context of the *murB* gene within the *dcw* cluster is unique to the *Bacillus* group and, taken together with our data, suggests that in these species it contributes to the optimal expression of cell division and PG biosynthetic functions during both vegetative growth and spore development.

Peptidoglycan (PG) is a critical component of the eubacterial cell envelope, providing mechanical resistance to withstand osmotic pressure (55) and functioning as a major determinant of cell shape, which ultimately also relies on topological information imposed by the actin cytoskeleton (6, 10, 33, 54). PG is also intimately involved in the cell division process and, in spore-forming bacteria, is additionally required for a cytoskeleton-like role during engulfment of the prespore by the mother cell, as well as for the formation of the spore cortex, a modified layer of PG, essential for spore heat resistance (reviewed in reference 17).

In all eubacteria examined to date, many of the genes involved in PG biosynthesis and cell division are grouped in the highly conserved *dcw* (for "division and cell wall") cluster (Fig. 1A). A correlation between bacterial cell shape and the arrangement of genes within the *dcw* cluster has been suggested (51). Specifically, it appears that rod-shaped bacteria have retained a more conserved and compact *dcw* cluster, and that transitions to other bacterial shapes have involved rearrangements and loss of gene order conservation within the cluster (51). Other features of the region appear to be associated with the biology of certain groups. Examples are the duplication of the *pbpB* gene to originate the *spoVD* gene in spore formers of the genus *Bacillus* (9, 11,

12) and the presence of a sporulation-specific gene, *spoVE*, instead of *ftsW*, which is located in a different chromosomal location. Also, the *spoVE-murG-murB-divIB* unit (Fig. 1A) appears restricted to this group and, among the *Bacillus* species whose genomes have been sequenced, is only absent from *B. clausii* (34, 35). Both *spoVE* and *spoVD* are transcribed during sporulation in the mother cell, from σᴱ-dependent promoters located just upstream of their coding regions, and both are dispensable for growth but essential for cortex biogenesis during spore formation (29, 42, 53).

In *B. subtilis* the *dcw* cluster is located in the 133° to 135° region of the chromosome (29). During vegetative growth, several genes in the cluster are cotranscribed in the form of long polycistronic messages, which appear to originate from promoters located just upstream of the *murE* gene, or even further upstream in the cluster (12, 25, 29). However, individual vegetative promoters have also been identified for specific genes or groups of genes, such as the *divIB* gene or the *pbpB* operon (12, 25). The *divIB* gene codes for a protein required for septum formation during both medial (vegetative) and asymmetric (sporulation) cell division (reference 45 and references therein). *divIB* is transcribed mainly from a promoter located upstream of *murE* but also from a weak σᴬ-type promoter located just 93 bp upstream of the *divIB* coding sequence (25, 45). Cells in which *murB* is separated from *divIB* by an integrational plasmid exhibit a defect in nucleoid structure and segregation and fail to activate Spo0A-dependent gene expression at the onset of sporulation (45). Moreover, they show a slight growth defect that is exacerbated upon expression

* Corresponding author. Mailing address: Instituto de Tecnologia Química e Biológica, Universidade Nova de Lisboa, Avenida da República, Apartado 127, 2781-901 Oeiras Codex, Portugal. Phone: 351-21-4469521. Fax: 351-21-4411277. E-mail: aoh@itqb.unl.pt.
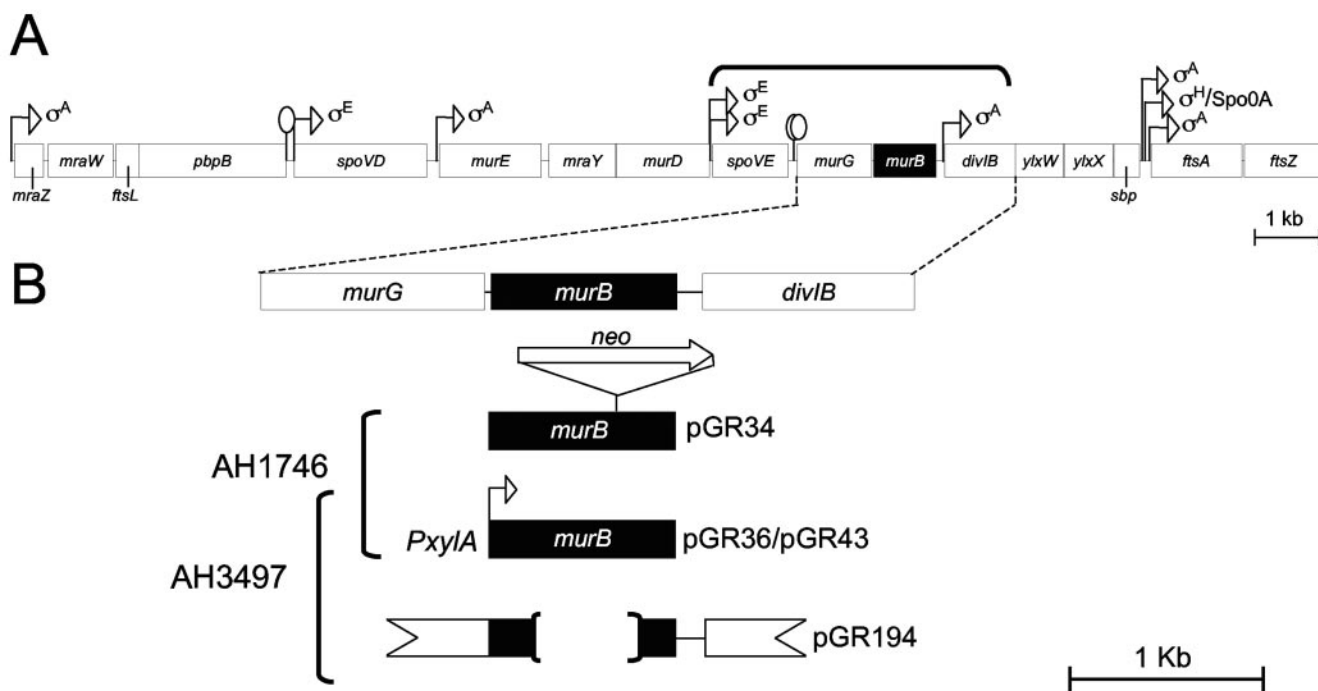
FIG. 1. Genetic organization of the *dcw* cluster in *B. subtilis*. (A) Location, extent, and orientation of the different genes present in the *dcw* cluster of *B. subtilis*. Sequences used in the construction of the figure were obtained from the SubtiList server (http://genolist.pasteur.fr/SubtiList/). The figure includes the positions of the transcriptional terminators (stem and loop structures) and main promoters (curved arrows) found in the region, with the regulators involved in their utilization indicated (12, 20, 21, 25, 29, 45). The horizontal bracket indicates the *spoVE-murG-murB-divIB* unit that appears to be unique to the *Bacillus* group of spore formers. (B) Region of the *dcw* cluster cloned to create pGR34 (used to create a *murB*::*neo* strain at the indicated position), pGR194 (used to create a Δ*murB* in-frame deletion, the boundaries of which are shown in the figure), pGR36, and pGR43 (used to integrate a xylose-inducible *murB* allele at *amyE*). The P*xylA-murB* allele was combined with the *murB*::*neo* and Δ*murB* alleles to create strains AH1746 and AH3497, respectively, as shown (see Materials and Methods for details).

of a second copy of the upstream *murB* gene (45). Together with the observation that the *spoVE-murG-murB-divIB* unit is conserved within bacteria of the genus *Bacillus* (Fig. 1), this observation suggests that coordinated expression of these genes may be important for normal growth. Moreover, because *murG* and *murB* appear to be cotranscribed from the σ^E-dependent promoter of *spoVE*, this linkage may also be important during sporulation (15).

Here, we have examined whether the chromosomal position of *murB* is important for its function. The *murB* gene codes for UDP-*N*-acetylenolpyruvoylglucosamine reductase, which is required at an early step in the PG biosynthetic pathway. The first step in PG biosynthesis involves the MurA enzyme, which catalyzes the production of UDP-*N*-acetylenolpyruvyl-glucosamine (UDPGlcNAcEP) from UDP-*N*-acetylglucosamine (UDP-GlcNAc) and phosphoenolpiruvate. The enolpyruvyl moiety is then reduced by MurB, yielding UDP-*N*-acetylmuramic acid (UDPMurNAc). A pentapeptide chain is then added onto UDPMurNAc by the sequential action of MurC, MurD, MurE, and MurF (16, 55). The resultant UDPMurNAc-pentapeptide is transferred to the membrane acceptor (undecaprenylphosphate) by the MraY transferase to form lipid I, and then *N*-acetylglucosamine (GlcNAc) is added by another transferase, MurG, to form lipid II. The GlcNAc-MurNAc(pentapeptide)-pyrophosphoryl-undecaprenol is next translocated across the membrane, where it is incorporated into nascent PG by the transglycosylase

and transpeptidation reactions catalyzed by several penicillin binding proteins (PBPs) (18).

The *murB* gene is essential in *Escherichia coli* and *Staphylococcus aureus*, as demonstrated by the isolation of temperature-sensitive mutants (38, 41, 44). Unsuccessful inactivation attempts also suggested its essentiality in *B. subtilis* (46). In this work, we have constructed and characterized a *murB* conditional mutant and have examined the effects of the ectopic expression of *murB*. We show that the *murB* gene is essential for normal growth, cell morphology, and resistance to cell wall-active antibiotics. We also show that normal expression of *murB* is required at the stage of spore cortex synthesis for the formation of heat-resistant spores. The evidence suggests that expression of *murB* from its normal locus within the *dcw* cluster is required for normal growth and efficient spore formation.

MATERIALS AND METHODS

Bacterial strains, media, and general methods. All of the *B. subtilis* strains used in this study are congenic derivatives of strain MB24 (*trpC2 metC3*) (Table 1). The *E. coli* strain DH5α (BRL) was used for plasmid construction and propagation (Table 1). Growth, selection, and maintenance of drug-resistant transformants of *E. coli* or *B. subtilis* was as described previously (27, 28). The high-fidelity *Pfu* polymerase (Stratagene, La Jolla, Calif.) was used to generate PCR fragments for cloning, which were sequenced to ensure that no mutations were introduced. Sporulation was induced by exhaustion in Difco sporulation medium (DSM) (8, 50), and its frequency was expressed as the percentage of heat-

TABLE 1. Bacterial strains and plasmids

Strain or plasmid	Genotype/phenotype	Origin/reference
E. coli strains		
DH5α	F⁻ *lacZ*ΔM15 Δ(*lacZYA-argF*)*U169*; wild type	Gibco BRL
BL21(DE3)pLysS	F⁻ *ompT hsdS* (r⁻ m⁻) *gal dcm* (DE3) pLysS; Cm^r	Stratagene
AH1646	F⁻ *ompT hsdS* (r⁻ m⁻) *gal dcm* (DE3) pLysS pGR28; Amp^r Cm^r	This work
AH3268	F⁻ *ompT hsdS* (r⁻ m⁻) *gal dcm* (DE3) pLysS pGR144; Amp^r Cm^r	This work
B. subtilis strains		
MB24	*trpC2 metC3*; wild type	Laboratory stock
SL666	*trpC2 spoVE85*	26
AH1744	*trpC2 metC3 amyE*::P*xylA-murB*(77-753); Neo^r	This work
AH1745	*trpC2 metC3 amyE*::P*xylA-murB*; Cm^r	This work
AH1746	*trpC2 metC3 murB*::*neo amyE*::P*xylA-murB*; Neo^r Cm^r	This work
AH3356	*trpC2 metC3 murB*::*neo amyE*::P*xylA-murB thrC*::P*spac-divIB*; Neo^r Cm^r Em^r	This work
AH3497	*trpC2 metC3* Δ*murB amyE*::P*xylA-murB*; Cm^r	This work
AH3505	*trpC2 metC3* Δ*murB amyE*::P*xylA-murB* sp β::P*gerE-lacZ*; Cm^r Em^r	This work
Plasmids		
pBEST501	*bla neo*	32
pMS38	*bla cm*	59
pDG364	*bla amyE*::*cm*	8
pMLK83	*bla amyE*::*gus neo*	36
pAH235	*bla amyE*::P*spoIIIG-gusA neo*	28
pAH256	*bla spec*	28
pMALc2	*bla malE*	New England Biolabs
pCR2.1-TOPO	*bla*	Invitrogen, La Jolla, CA
pGEM T Easy	*bla*	Promega
pGR28	*bla malE-murB*	This work
pGR29	*bla* P*xylA*	This work
pGR34	*bla murB*::*neo*	This work
pGR35	*bla amyE*::P*xylA-gusA neo*	This work
pGR36	*bla amyE*::P*xylA-murB*(77-753) *neo*	This work
pGR40	*bla amyE*::P*xylA neo*	This work
pGR43	*bla murB*(301-1597) *cm*	This work
pGR46	*bla murB*(77-753)	This work
pGR63	*bla amyE*::P*spac-divIB neo*	45
pGR144	*bla malE-divIB*	This work
pGR163	*bla thrC*::P*spac-divIB erm*, *spec*	This work
pGR194	*bla* Δ*murB*	This work

resistant CFU relative to the total cell count (27). Spores were purified on step gradients of Gastrografin (Schering) (26, 27, 47).

Purification of MurB and DivIB fusion proteins for antibody production. The *murB* gene was PCR amplified from MB24 using primers *murB*-235D (5′-ATG GAGAAAGTGATACAGG-3′) and *murB*-1165R (5′-GCTTCAGTCTAGAAC TTGAATCAGCG-3′). The 930-bp product was cut with XbaI and inserted between the XmnI and XbaI sites of pMAL-c2 (New England Biolabs) to yield pGR28. The *divIB* gene (lacking the sequence for its transmembrane domain) was PCR amplified from MB24 using primers *divIB*-239D (5′-GCGGAGATC TGAGTTTTGGAGTTTGGAC-3′) and *divIB*-908R (5′-CCAAGCTTCCGT CTCAGCCGCGC-3′). The 669-bp product was digested with BglII and EcoRI and inserted between the BamHI and EcoRI sites of pMAL-c2 to create pGR144. pGR28 or pGR144 was introduced into *E. coli* BL21(DE3) (pLysS) (Novagen). The transformed cells were grown in 1 liter of LB to an optical density at 600 nm (OD$_{600}$) of 0.6 and induced with 5 mM isopropyl-β-D-thio-galactopyranoside (IPTG) for 2 h. The cells were collected and lysed as described previously (48). The lysate was clarified by centrifugation (30,000 × *g* for 30 min at 4°C) and applied to a 20-ml amylose column (New England Biolabs) equilibrated in lysis buffer. Column washing and elution were as described by the manufacturer. Purified MurB and DivIB fusion proteins were used to raise rabbit polyclonal antibodies (Eurogentec, Herstal, Belgium).

Immunoblot analysis. Samples (10 ml) of LB or DSM cultures were collected and lysed as described before (48). Samples (20 μg) of total protein were resolved on 12% or 15% polyacrylamide gels containing sodium dodecyl sulfate and subjected to immunoblot analysis as described previously (48). Antibodies were used at the following dilutions: anti-MurB, dilution of 1:1,000; anti-DivIB, 1:100; anti-β′ subunit of RNA polymerase (a gift from Bill Haldenwang), 1:250. A rabbit secondary antibody conjugated to horseradish peroxidase (Sigma) and

a mouse secondary antibody were used at dilutions of 1:10,000 and 1:200, respectively. The immunoblots were developed with enhanced chemiluminescence reagents (Amersham Pharmacia Biotech).

Construction of a *murB* conditional mutant. For construction of a *murB* conditional mutant, first a PCR fragment carrying the *xylA* promoter was produced using primers *xylR*-61D (5′-CTATTTTAGAATTCCTTTTTCATATTGAG-3′) and *xylR*-1558R (5′-GGAATGAGATCTGAGCCATGTGATTTCCC-3′) and digested with AflIII and BglII, and the 400-bp fragment was inserted into BssHII- and BglII-cut pAH256 (28), yielding pGR29. Then, the P*xylA* fragment was released from pGR29 with SpeI and XhoI and inserted between the SpeI and SalI sites of pAH235 (28), originating pGR35. Cleavage of pGR35 with EcoRI followed by religation produced pGR40. Next, a PCR fragment containing the first 246 codons of *murB*, obtained with primers *murB*-77D (5′-CTGATTGAAGCACTA GTCCGGATTGTAC-3′) and *murB*-753R (5′-GTAGCTGGGATCCATCTG CTCATTTGTC-3′), was inserted into pCR2.1-TOPO (Invitrogen, La Jolla, CA) to give pGR46, released from this plasmid with SpeI and EcoRI, and introduced between the same sites of pGR40, to yield pGR36 (Fig. 1B). AH1744 (AmyE⁻) resulted from the transformation of MB24 to neomycin resistance (Nm^r) with PstI-linearized pGR36. A plasmid (pGR43, Fig. 1B) containing the 3′ end of *murB* was made by inserting an NruI- and SphI-cut PCR product obtained with primers *murB*-213D (5′-GCAAGATCTAATGCGAGGTTACGATGGAG-3′) and *murB*-1597R (5′-GGTGTTTGCATGCACACAATGATCAGCACC-3′) between the same sites of pDG364 (8). PstI-cut pGR43 was used to transform AH1744 to chloramphenicol resistance (Cm^r). This generated AH1745 (Neo^s AmyE⁻), in which the presence of *murB* under P*xylA* control at *amyE* was verified by PCR and sequence analysis. A Neo^r determinant released from pBEST501 (32) with SmaI was introduced into SmaI-cut pGR28 to give pGR34 (Fig. 1B). ScaI-cut pGR34 was used to transform AH1745 to Nm^r in the presence
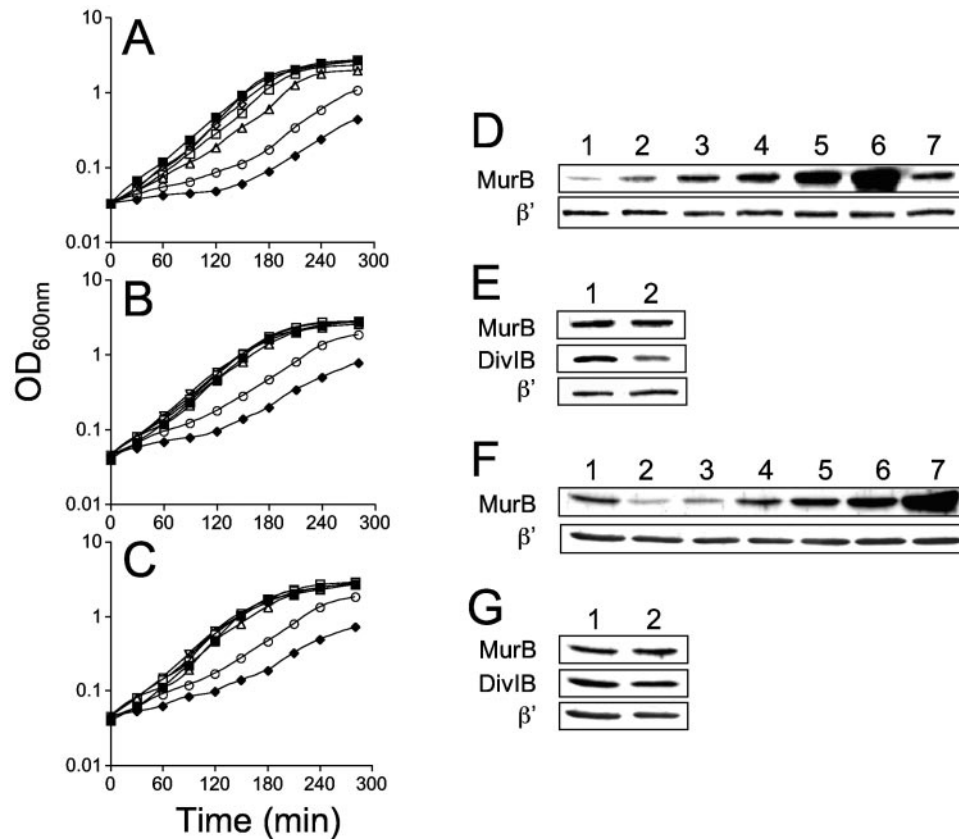
FIG. 2. Inducer-dependent growth and levels of MurB in P*xylA-murB* conditional mutants. (A) Growth of wild-type strain MB24 (filled squares) or AH1746 (Δ*murB*::*neo amyE*::P*xylA-murB*) in the absence of xylose (filled diamonds) or in the presence of increasing xylose concentrations, as follows: 0.001%, open circles; 0.0025%, open triangles; 0.005%, open squares; 0.01%, open diamonds; 0.1%, open inverted triangles. (B) Growth of MB24 (filled squares) or AH3356 (*murB*::*neo amyE*::P*xylA-murB thrC*::P*spac-divIB*) in the presence of 0.5 μM IPTG and in the absence of xylose (filled diamonds) or in the presence of xylose concentrations, as follows: 0.001%, open circles; 0.0025%, open triangles; 0.005%, open squares; 0.01%, open diamonds; 0.1%, open inverted triangles. (C) Growth of strain MB24 (filled squares) or AH3497 (Δ*murB amyE*::P*xylA-murB*) in the absence of xylose (filled diamonds) or in the presence of increasing xylose concentrations, as follows: 0.001%, open circles; 0.0025%, open triangles; 0.005%, open squares; 0.01%, open diamonds; 0.1%, open inverted triangles. Xylose (at all concentrations tested) or IPTG did not influence the growth rate of the wild-type strain, whose growth is represented in the absence of either inducer. (D and F) Immunoblot analysis using anti-MurB and anti-β′ subunit of the RNA polymerase antisera (Material and Methods) of mid-log-phase samples of cultures of MB24 (lane 7 in panel D and lane 1 in panel F) and AH1746 (panel D, lanes 1 to 6) or AH3497 (panel F, lanes 2 to 7), as represented in panels A and C. Lanes in panels D are as follows: lane 1, strain AH1746 grown in the absence of xylose; lane 2, 0.001% xylose; lane 3, 0.0025% xylose; lane 4, 0.005% xylose; lane 5, 0.01% xylose; lane 6, 0.1% xylose; lane 7, MB24 (no xylose). Lanes in panel F are as follows: lane 1, strain MB24 grown in the absence xylose; lanes 2 to 7, strain AH3497 grown in the absence or presence of xylose (lane 2, no xylose; lane 3, 0.001% xylose; lane 4, 0.0025% xylose; lane 5, 0.005% xylose; lane 6, 0.01% xylose; lane 7, 0.1% xylose). (E and G) Samples of the above cultures of MB24, AH1746, or AH3497 were subject to immunoblot analysis using anti-MurB, anti-DivIB, and anti-β′ RNA polymerase subunit antisera (see Materials and Methods). (E) Lane 1, MB24 (wild type); lane 2, AH1746 grown in the presence of 0.0025% xylose. (G) Lane 1, MB24 (wild type); lane 2, AH3497 grown in the presence of 0.0025% xylose.

of 0.1% xylose. This produced AH1746, in which inactivation of *murB* within the *dcw* region was verified by PCR.

Construction of an inducible *divIB* allele. The P*spac-divIB-lacI* region in pGR90 (45) was PCR amplified with primers pDH45D (5′-GAAGTGGTCAAG AATTCACTAGGCAC-3′) and pDH1685R (5′-GAAGATCTTCACATTAAT TGCGTTGCGCTCACTG-3′), and the product was cut with EcoRI and BglII and inserted between the EcoRI and BamHI sites of pDG1664 (24), to yield pGR163. Plasmid pGR163 was used to transform MB24 selecting for Em^r, to produce AH3303 (Table 1) in which P*spac-divIB-lacI* resides at *thrC*, as verified by PCR. Chromosomal DNA from AH3303 was used to transform AH1746 to Em^r. A transformant was selected and named AH3356 (Table 1).

In-frame deletion of *murB*. First, two PCR products of 600 bp encompassing the 5′ and 3′ regions of *murB* were produced using primers *murB*-77D (see above) and *murB*faseR(BglII) (5′-GCTCATATCAGATCTGTGAGCGCCGGC-3′) and primers *murB*faseD(BglII) (5′-CGTGAAAGATCTGAGATTGATATG CACACAGAG-3′) and *divIB*430R(EcoRI) (5′-CTGAGCCGAATTCAAGCA CTTCATAGTAC-3′). The two products were digested with BglII, ligated to-

gether, and inserted into pGEM-Teasy (Promega). This created pGR194 (Fig. 1B), which was used with pDG1731 (24) to cotransform AH1745 to spectino-mycin resistance (Sp^r). One erythromycin-susceptible transformant (AH3497) was dependent on xylose for growth and had a *murB* 447-bp in-frame deletion, as verified by PCR and sequence analysis.

Microscopy. Culture samples were collected and stained with the membrane dye FM4-64 (Molecular Probes), as described previously (45). Phase-contrast or fluorescence images were acquired in a Leica DMRA2 microscope coupled to a CoolSNAP HQ Photometrics camera (Roper Scientific).

Antimicrobial susceptibility. Susceptibility to antibiotics was determined by measuring bacterial growth on square gradient plates (12 cm by 12 cm) as described previously (2, 7). Briefly, each plate contained LB agar supplemented with 0.001%, 0.005%, 0.01%, or 0.1% xylose (50 ml in each of the top and bottom layers). Antibiotics used for the top layer were as follows: vancomycin, 0.25 μg ml^−1; oxacillin, 0.2 μg ml^−1; fosfomycin, 20 μg ml^−1; D-cycloserine, 10 μg ml^−1; cephalosporin, 10 μg ml^−1. Strains were grown in LB (supplemented with 0.0025% xylose when required) for ~16 h, diluted 100-fold into LB supple-

mented with 0.01% xylose, and incubated at 37°C to an OD_{600} of 0.2. Cell plating was as described previously (1, 22, 23). Confluent growth along the gradient was scored after 18 h at 37°C.

RESULTS

***murB* is essential in *B. subtilis*.** Previous unsuccessful attempts to insertionally inactivate the *murB* gene in *B. subtilis* were interpreted as indicating its essentiality (46). Here, we constructed a *murB* conditional mutant by first inserting a copy of *murB* under the control of the xylose-inducible P*xylA* promoter at the nonessential *amyE* locus and then by using the *murB* merodiploid (AH1745) to disrupt the *murB* gene at its normal locus, by insertion of a Nm^r cassette within the gene's coding sequence. Attempts to obtain Nm^r transformants of AH1745 in the absence of xylose failed, but those readily arose when the medium was supplemented with 0.1% xylose. One, in which the *murB* gene was shown to be inactivated, was designated AH1746 (Table 1). To test the effect of varying the expression level of *murB* on cell growth, overnight cultures of AH1746 grown in the presence of 0.05% xylose were centrifuged, washed with LB medium, resuspended in xylose-free medium, and diluted to an OD_{600} of 0.02 in prewarmed LB medium without xylose or supplemented with increasing concentrations of inducer. The growth rate of the cultures was determined by monitoring the rate of increase in the OD_{600}. In parallel, we monitored the levels of MurB in cells of the conditional mutant using an anti-MurB antibody (see Materials and Methods).

As shown in Fig. 2A, the growth rate of the *murB* conditional mutant (AH1746) was proportional to the concentration of xylose in the medium. The wild-type strain exhibited a doubling time of about 30 min in LB medium at 37°C in the absence or in the presence of 1% xylose, whereas the doubling time of the *murB* conditional mutant in the absence of inducer was of 93.1 min (Table 2). Residual growth of the mutant in the absence of xylose is presumably caused by leakiness of the P*xylA* promoter, allowing MurB to accumulate to about 30% of the level in the wild-type strain (Fig. 2D; compare lanes 1 and 7). Increasing the concentration of xylose in the medium led to an increment in the growth rate, in parallel with an increase in the cellular level of MurB (Fig. 2D). Note that as a control for these experiments, the same membranes were probed with an antibody against the β′ subunit of RNA polymerase, whose levels remained constant regardless of the xylose concentration and similar to those in the wild-type strain MB24 (Fig. 2D). As shown in Fig. 2D, at a xylose concentration of 0.0025%, MurB accumulated to wild-type levels (compare lanes 3 and 7), but surprisingly the growth rate of this culture was lower than that of wild-type cells, with a doubling time of 37.3 min compared to 30.1 min for the wild type (Table 2). A xylose concentration of 0.01% restored a wild-type growth rate (doubling time of about 30 min) to the conditional mutant (Fig. 2A and Table 2). However, under these conditions MurB accumulated to levels about three times higher than in the wild-type strain (Fig. 2D; compare lanes 5 and 7).

A link between *murB* and *divIB*. The separation of the *murB* and *divIB* genes by an integrational plasmid produced a strain with a slow growth phenotype, which could be corrected by a copy of *divIB* in *trans* (45). In that mutant, *divIB* was tran-

TABLE 2. Growth rates of the *murB* conditional
mutant in LB medium

Strain	Relevant genotype	% Xylose[a]	Doubling time (min)[b]
MB24	Wild type	0	30.1 ± 2.2
		1	30.9 ± 1.7
AH1746	Δ*murB*::*neo amyE*::P*xylA-murB*	0	93.1 ± 5.4
		0.001	69.2 ± 3.1
		0.0025	37.3 ± 3.2
		0.005	35.2 ± 2.7
		0.01	**30.0 ± 3.3**
		0.1	30.9 ± 1.2
		1	29.0 ± 2.4
AH3356	Δ*murB*::*neo amyE*::P*xylA-murB* *thrC*::P*spac-divIB*(+)	0	89.0 ± 4.2
		0.001	63.0 ± 4.7
		0.0025	**30.6 ± 3.4**
		0.005	30.1 ± 3.1
		0.01	30.8 ± 4.1
		0.1	30.9 ± 2.2
		1	28.6 ± 1.7
AH3497	Δ*murB amyE*::P*xylA-murB*	0	88.1 ± 6.2
		0.001	53.1 ± 6.8
		0.0025	**30.1 ± 2.3**
		0.005	29.1 ± 1.3
		0.01	30.1 ± 1.6
		0.1	30.5 ± 1.2
		1	30.5 ± 1.7

[a] The numbers in bold are the minimum xylose concentration at which a wild-type doubling time is observed.
[b] Data are averages from three independent experiments. IPTG, for induction of *divIB*, was added at a concentration of 0.5 μM.

scribed only from a weak σ^A-type promoter located just upstream of the gene (45). To test whether the Neo^r cassette inserted into *murB* affected the levels of DivIB, we conducted immunoblot analysis with an anti-DivIB antibody (see Materials and Methods). We examined the levels of DivIB in strain AH1746 during the exponential phase of growth in the presence of 0.0025% xylose, which permits MurB to accumulate to wild-type levels (see above). The results in Fig. 2E indicate that the levels of DivIB in AH1746 were slightly reduced (by about 10%) relative to MB24 (wild type), while the levels of MurB or of the β′ subunit of RNA polymerase remained unchanged in the two strains (Fig. 2E). The reduction in the levels of DivIB was not sufficient to cause any discernible effect on cell division, as the cell length distribution was similar to that of the wild-type strain (data not shown; see also reference 45).

To test whether the requirement for higher than wild-type levels of MurB for normal growth of AH1746 was due to reduced levels of DivIB, we placed a second copy of *divIB* under the control of the IPTG-inducible P*spac* promoter at the nonessential *thrC* locus. The resulting strain, AH3356 (Δ*murB*::*neo amyE*::P*xylA-murB thrC*::P*spac-divIB*), was, like its parent, xylose dependent for growth (not shown). However, in the presence of 0.5 μM IPTG and 0.001% xylose, the doubling time of AH3356 was 63 min, compared to 93 min for AH1746 (Fig. 2B and Table 2). Moreover, in the presence of 0.5 μM IPTG, a wild-type doubling time was observed for AH3356 at a xylose concentration of only 0.0025%; that is, four times lower than for the parental strain AH1746 (Table 2; see also above). Thus, the need for increased levels of MurB to sustain a normal growth rate in AH1746 results from the re-
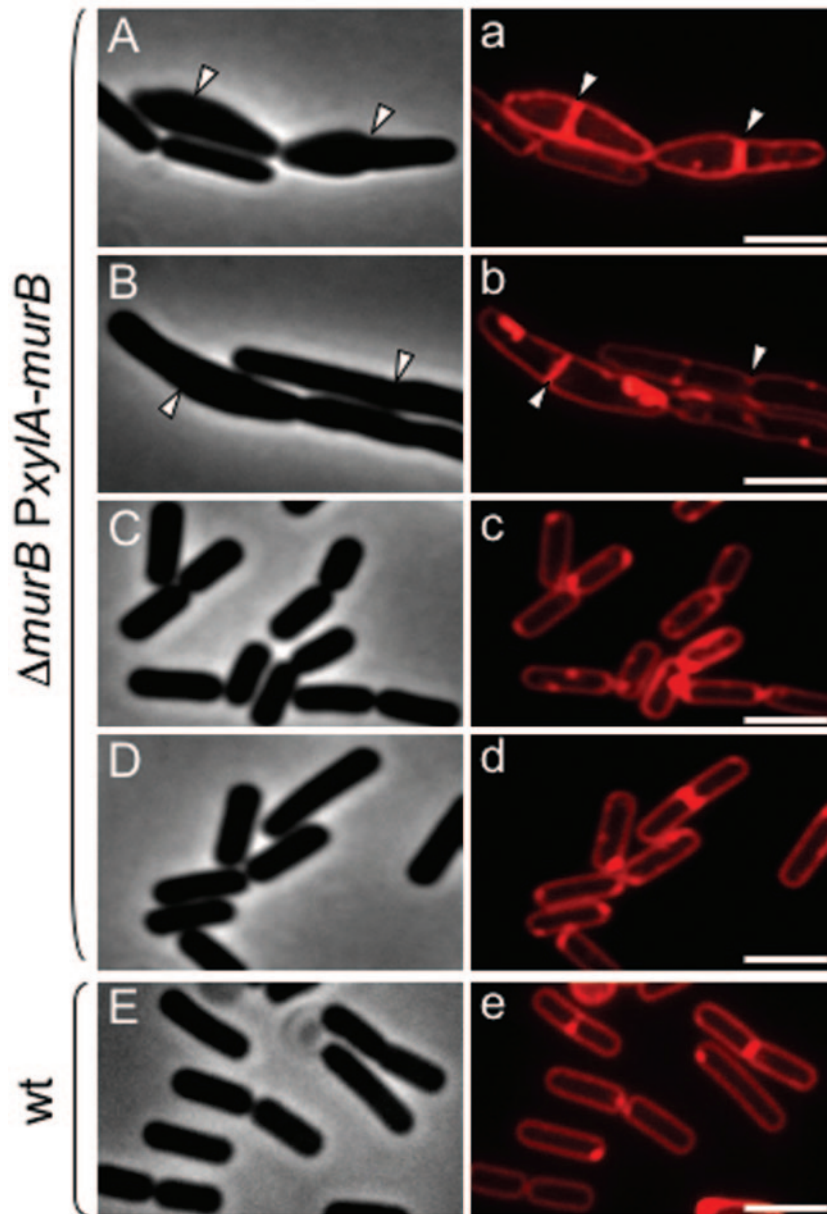
FIG. 3. MurB depletion causes a defect in cell morphology. The figure depicts the morphology of cells in LB cultures of the wild-type (wt) strain MB24 and AH3497 ($\Delta murB$ $amyE$::P$xylA$-$murB$). (A/a through D/d) Cells from strain AH3497 grown in the absence of xylose (A/a) or in the presence of 0.001% xylose (B/b), 0.01% xylose (C/c), or 0.1% xylose (D/d). (E/e) MB24 cells. The cells were harvested during the exponential phase of growth and stained with the membrane dye FM4-64 to allow visualization of membranes and septa for observation by phase-contrast microscopy (A to E) and by fluorescence microscopy (a to e). Arrowheads point to bulges close to division septa. Scale bars, 2 μm.

duction in DivIB levels; conversely, increased expression of *divIB* reduces the requirement for MurB.

A nonpolar *murB* in-frame deletion mutant. Because of the effect of the *murB*::*neo* allele on the levels of DivIB, we constructed an in-frame deletion of the *murB* gene (see Materials and Methods) and transferred the new allele into strain AH1745. The new conditional mutant, AH3497, exhibited xylose dependency for growth (Table 2). AH3497 grew slowly, with a doubling time of 88.1 min in the absence of inducer (Table 2 and Fig. 2C). However, in contrast to AH1746 (*murB*::*neo*), which grew normally at a xylose concentration of 0.01%, AH3497 showed the

same doubling time as the wild type in the presence of only 0.0025% xylose (Table 2 and Fig. 2C), a concentration at which AH3356 (*murB*::*neo* P*spac*-*divIB*) also exhibited normal growth. As for AH1746, the level of MurB, but not that of the β′ subunit of RNA polymerase, increased with the concentration of xylose in the growth medium (Fig. 2F). For AH3497 growing in the presence of 0.0025% xylose, MurB accumulated to wild-type levels (Fig. 2F, lanes 1 and 4, and Fig. 2G), and the doubling time was 30.6 min, similar to that of the wild type (30.1 min; Fig. 2C and Table 2). Moreover, under these conditions, DivIB accumulated to wild-type levels, as shown by the immunoblot analysis docu-
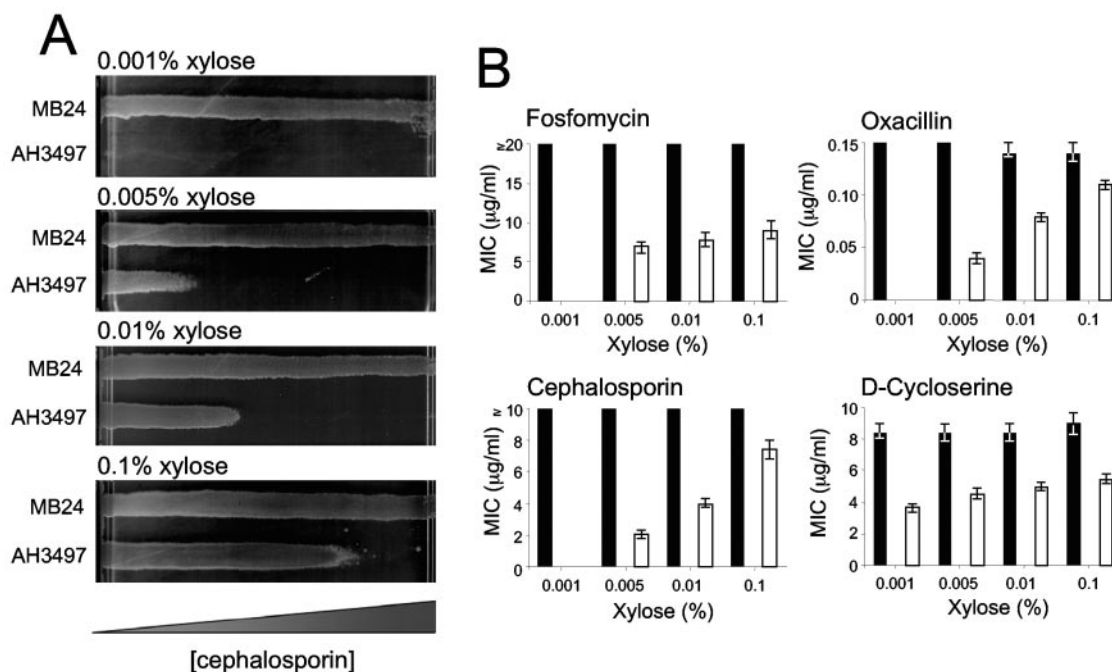
FIG. 4. The *murB* conditional mutant shows increased susceptibility to cell wall-active antibiotics. (A) Susceptibility of MB24 (wild type) and AH3497 (Δ*murB amyE*::P*xylA-murB*) to the antibiotic cephalosporin when grown in increasing concentrations of xylose. (B) Quantification of the susceptibility of strains MB24 (black columns) and AH3497 (white columns) to the indicated antibiotics as a function of the xylose concentration, as determined on antibiotic gradient plates (as depicted in panel A). Susceptibility is shown as the MIC of antibiotic (as defined in Materials and Methods) relative to the level of xylose present in the gradient plates. The graphs shown represent averages of three independent experiments; error bars show standard deviations.

mented in Fig. 2G, where probing of the same membranes with an anti-MurB and with an anti-RNA polymerase β′ subunit antibody confirmed equivalent loadings. The results show that the in-frame deletion of *murB* has no impact on the levels of DivIB, and accordingly the conditional mutant exhibited a normal growth rate at wild-type levels of MurB.

Morphology of the *murB* conditional mutant. To examine whether growth of AH3497 in the absence of xylose or in the presence of low levels of inducer caused alterations in cell shape, cells in mid-log-phase cultures of the conditional mutant were examined by fluorescence and phase-contrast microscopy. We found that in the absence of inducer, approximately 30% of the cells were slightly elongated and showed bulges, often at one end of the cell, close to a division septum (Fig. 3A and a, arrowheads). Occasionally, what looked like empty vesicles bulged out from the cells, and many cells were lysed (data not shown). Induction of the xylose promoter with 0.001% xylose reduced the frequency of bulge formation to 17%, and when these appeared (Fig. 3B and b, arrowheads), they were not as pronounced as in the absence of inducer. Cell swelling has been observed for other *B. subtilis* mutants with lesions affecting the expression of genes essential for PG biosynthesis. For example, low levels of expression of the *rodA* morphogene, essential for cell elongation, causes swelling and lysis (30), as does inactivation of the genes coding for PBP2a and PBPH, which are partially redundant functional homologues of the *E. coli* elongation-specific PBP2 (11, 57, 58).

Xylose concentrations of 0.0025% (not shown) or higher restored normal length and cell shape to the *murB* conditional

mutant AH3497 (Fig. 3C through d). Addition of 0.01% xylose to cells growing in the absence of inducer restored normal cell morphology, suggesting that the cell envelope deficiency could be overcome if expression of *murB* was restored (Fig. 3C through d). The average cell length of the population in the presence of 0.01% (3.12 μm ± 0.75) or 0.1% (3.26 μm ± 0.65) xylose, concentrations at which no alteration of cell shape was noticed, did not significantly differ from that of a wild-type population (3.55 μm ± 0.88). We infer from these results that expression of *murB* is required for normal cell shape. Also, in agreement with earlier work (10, 30, 33, 56, 57), the results also suggest a correlation between a normal growth rate and the acquisition of rod-shaped morphology by *B. subtilis* cells.

Cells depleted for MurB show increased susceptibility to antibiotics. Strains engineered for low-level expression of single essential genes, and thus rendered hypersensitive to inhibitors of the corresponding gene product, have been used in screens for new antimicrobial compounds (13). No MurB inhibitors with antimicrobial activity were available to us (49), but we tested whether MurB depletion could cause hypersensitivity to several other cell wall-active antibiotics. The tests were performed on gradient plates (2, 7) containing the antibiotics fosfomycin, D-cycloserine, oxacillin, vancomycin, and cephalosporin, supplemented with increasing concentrations of xylose (from 0.001 to 0.1%; see Materials and Methods). Under these conditions, the extent of the zone of growth is a function of the resistance level of the strain (Fig. 4A), and the MIC is defined as the lowest concentration of antibiotic that prevents growth (37). The results in Fig. 4B show that while
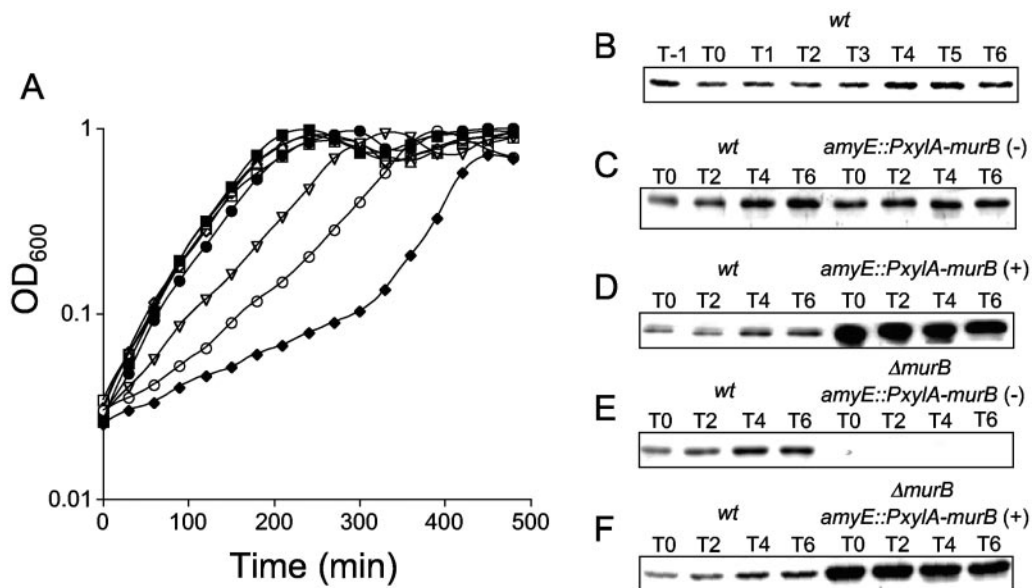
FIG. 5. Effect of MurB depletion during growth and sporulation in DSM medium. (A) Overnight cultures of the wild-type strain MB24 (filled squares) and of AH3497 (Δ*murB amyE*::P*xylA-murB*) in LB medium, later grown in the presence of 0.0025% xylose, were centrifuged to collect the cells. These were washed with DSM medium, resuspended in xylose-free DSM, and used to inoculate prewarmed DSM to an OD_{600} of 0.02 in the absence of xylose (filled diamonds) or in the presence of xylose at the following concentrations: 0.0005%, open circles; 0.001%, open inverted triangles; 0.0025%, filled circles; 0.005%, open triangles; 0.01%, open diamonds; 0.1%, open squares. Growth of the cultures was followed by monitoring of the rate of increase in OD_{600} through time (in minutes) following inoculation. Note that some cultures reach stationary phase, defined as the initiation of sporulation (T0), at different times. (B through F) Cells of the wild type (wt) (MB24), AH1745 (*amyE*::P*xylA-murB*), or AH3497 (Δ*murB amyE*::P*xylA-murB*) were grown as described above and collected at different times during growth and sporulation to monitor the levels of MurB using an anti-MurB antibody. Panel B shows the levels of MurB in the wild-type strain MB24. Panels C to F compare the levels of MurB in MB24, AH1745, and AH3497 grown in the absence of xylose (−) or in the presence of 0.1% xylose (+). The numbers above each lane represent time (in hours) before or after the onset of sporulation (T0).

xylose did not influence the resistance of the wild-type strain MB24, the *murB* conditional mutant AH3497 was more susceptible to the antibiotics fosfomycin, oxacillin, D-cycloserine, and cephalosporin at all the concentrations of xylose tested. However, while the resistance to oxacillin and cephalosporin clearly augmented in parallel with the increase in xylose concentration in the medium, the resistance of AH3497 to fosfomycin and D-cycloserine was much less pronounced. Also, even at a xylose concentration of 0.1%, which permits the accumulation of MurB to levels almost 15 times higher than in the wild type (Fig. 2E; also see above), wild-type levels of resistance were never achieved (Fig. 4A and B). In contrast, the *murB* conditional mutant was found to be less susceptible to vancomycin, chloramphenicol, or tetracycline at any xylose concentration tested (data not shown). Fosfomycin is an inhibitor of MurA, the UDP-GlcNAc enolpyruvyl transferase that catalyzes the first committed step in the synthesis of PG, and acts just upstream of MurB in the pathway (16, 49). MurA and MurB act sequentially to convert UDP-GlcNac into UDP-MurNAc. D-Cycloserine is a competitive inhibitor of alanine racemase (Alr) and of D-alanine:D-alanine ligase (Ddl) (16, 49). Alr and Ddl act sequentially to produce D-ala-D-ala, which is then added to UDP-MurNAc tripeptide by the MurF lyase (16, 49). Oxacillin and cephalosporin are β-lactam antibiotics that interfere with PG synthesis by inhibiting the final transpeptidation needed for the cross-linking of the PG molecules (49) Thus, a reduction in the level of expression of the *murB* gene does not cause a generalized hypersensitivity of the cells to antibiotics.

Rather, the enzymatic steps catalyzed by MurA, and by Alr or Ddl in the cytoplasm, and the transpeptidation step that takes place at the cell wall become more sensitive to inhibition by specific antibiotics, when the level of expression of *murB* is altered.

MurB levels throughout sporulation. Formation of heat-resistant spores involves the synthesis of a layer of modified PG known as the spore cortex (3, 18, 43). Synthesis of the spore cortex is likely to involve most of the vegetative components of the PG-synthesizing machinery, although it also requires the expression of several sporulation-specific genes (3, 18). Here, we used an anti-MurB antibody to examine the profile of accumulation of MurB during sporulation. For that we grew the wild-type strain MB24 in DSM medium, in which sporulation is induced by nutrient exhaustion, and took samples during growth, at the onset of the stationary phase of growth (defined as the initiation of sporulation), and at various intervals thereafter for immunoblot analysis. The results in Fig. 5B show that the levels of MurB appeared to decrease as cells approach the end of the exponential phase of growth in DSM and that the decline in MurB levels persisted until about 1 h after the onset of sporulation (Fig. 5B). The levels of MurB then appear to steadily increase until at least hour 6 of sporulation (Fig. 5B). Synthesis of the spore cortex follows the activation of the late mother cell regulator σ^K, which takes place around hour 4 of sporulation (17, 18, 43). Thus, the levels of MurB appear to coincide with the time of synthesis of the spore cortex. The increase in the level of MurB during sporulation is consistent with the results of a recent study suggesting that the transcrip-

TABLE 3. Sporulation of a *murB* conditional mutant in DSM medium

Strain	Relevant genotype	% Xylose	Viable cell count	Heat-resistant cell count	% Sporulation
MB24	Wild type	0	6.7×10^8	7.0×10^8	100
		0.001	6.8×10^8	6.7×10^8	97.8
		0.01	6.9×10^8	6.8×10^8	98.5
		1	7.1×10^8	6.9×10^8	97.1
AH1745	*amyE*::P*xylA-murB*	0	5.6×10^8	5.4×10^8	96.4
		0.001	5.5×10^8	5.3×10^8	96.3
		0.01	6.7×10^8	6.4×10^8	95.5
		1	6.9×10^8	6.4×10^8	92.7
AH3497	Δ*murB amyE*::P*xylA-murB*	0	7.7×10^7	1.6×10^4	0.02
		0.001	5.5×10^7	1.7×10^4	0.03
		0.01	6.3×10^8	1.4×10^4	0.002
		1	6.4×10^8	1.3×10^4	0.002

tion of both *murG* and *murB* is enhanced during sporulation, presumably from the sporulation-specific *spoVE* promoter (14, 15) (Fig. 1). Presumably, increased transcription of *murB* is required to increase the levels of MurB at the time of cortex formation.

We then examined the impact of varying the expression level of *murB* from the P*xylA* promoter on the efficiency of sporulation in DSM. Under the conditions used, the Spo$^+$ strain MB24 produced 6.7×10^8 to 7.0×10^8 spores per ml of culture, independently of the level of xylose present in the sporulation medium (Table 3). In the absence of xylose, AH3497 (Δ*murB* P*xylA-murB*) was still able to grow, albeit slower than the wild type, entered stationary phase at an OD$_{600}$ slightly lower than a culture of the wild type (Fig. 5A), and formed only about 10^4 spores per ml of culture (Table 3). At xylose concentrations of 0.0005% or 0.001%, AH3497 grew slower than the wild type in DSM, but at xylose concentrations of 0.0025% or higher (up to 0.1%), AH3497 showed a wild-type growth rate in DSM (Fig. 5A). However, at all xylose concentrations tested, AH3497 was impaired in the formation of heat-resistant spores, with titers in the range of 10^4 per ml of culture (Table 3). The reduced sporulation efficiency was not caused by addition of xylose, because a *murB*$^+$ strain (AH1745) harboring an extra copy of *murB* under the control of P*xylA* at *amyE* sporulated at wild-type levels regardless of the xylose concentration in the medium (Table 3).

To test whether the failure of AH3497 to sporulate efficiently could be due to insufficient levels of MurB, samples of DSM cultures in the absence or in the presence of 0.1% xylose (the highest concentration tested) were collected throughout sporulation, and the levels of MurB were analyzed by immunoblot analysis. The results in Fig. 5E show that no MurB could be detected throughout sporulation of AH3497 in DSM in the absence of inducer. In the presence of 0.1% xylose, however, the levels of MurB at the onset of sporulation (T0) were much higher than for the wild type and remained higher than for the wild type throughout sporulation (Fig. 5F). Therefore, the failure of AH3497 to sporulate efficiently in the presence of 0.1% xylose is not due to reduced levels of MurB during sporulation. Conversely, the sporulation phenotype of AH3497 also does not appear to be due to increased levels of MurB. We base this inference on the observation that in

AH1745 (*murB*$^+$ P*xylA-murB*) grown in the presence of 0.1% xylose (a condition under which the strain sporulates efficiently; Table 3), the levels of MurB during sporulation were also elevated relative to the wild type (Fig. 5D), at least to the same extent of the increase in AH3497 (Fig. 5F). We propose that the sporulation phenotype of AH3497 is due to the ectopic expression of *murB* in this strain.

Sporulating cells of the *murB* conditional mutant are blocked at the stage of cortex formation. In an attempt to determine the stage in the sporulation pathway at which AH3497 was blocked, spores from cultures of the *murB* conditional mutant growing in the absence or in the presence of increasing concentrations of xylose were purified 24 h after the onset of sporulation and observed under phase-contrast microscopy. Approximately 97% of the spores produced by the wild-type strain (Fig. 6A) or by AH1745 (*murB*$^+$ P*xylA-murB*) (not shown) were bright phase, independently of the amount of xylose present in the medium. In contrast, almost 99% of spores of the *murB* conditional mutant grown in the absence and presence of increasing concentrations of inducer were dark phase (Fig. 6B through F). Dark-phase immature spores were seen inside the mother cell or as free "sporelets" in the culture medium. The production of dark-phase, immature spores is a characteristic of mutants with lesions in genes involved in the synthesis of the spore cortex PG (29). These results suggest that the ectopic expression of *murB* fails to promote efficient synthesis of the spore cortex and hence to support formation of heat-resistant spores.

DISCUSSION

In an extension of earlier work (46), the results herein presented indicate that expression of the *murB* gene is essential for normal growth and cell shape in *B. subtilis*. We base this conclusion on the analysis of two different *murB* conditional mutants, in which the only functional copy of the gene was placed under the control of the xylose-inducible P*xylA* promoter at the nonessential *amyE* locus. In one mutant (AH1746), the *murB* gene present in the *dcw* cluster was insertionally inactivated. In the second (AH3497), an in-frame deletion was introduced into *murB* in the *dcw* cluster. The two strains exhibited slow growth in the absence of inducer and greatly altered cell
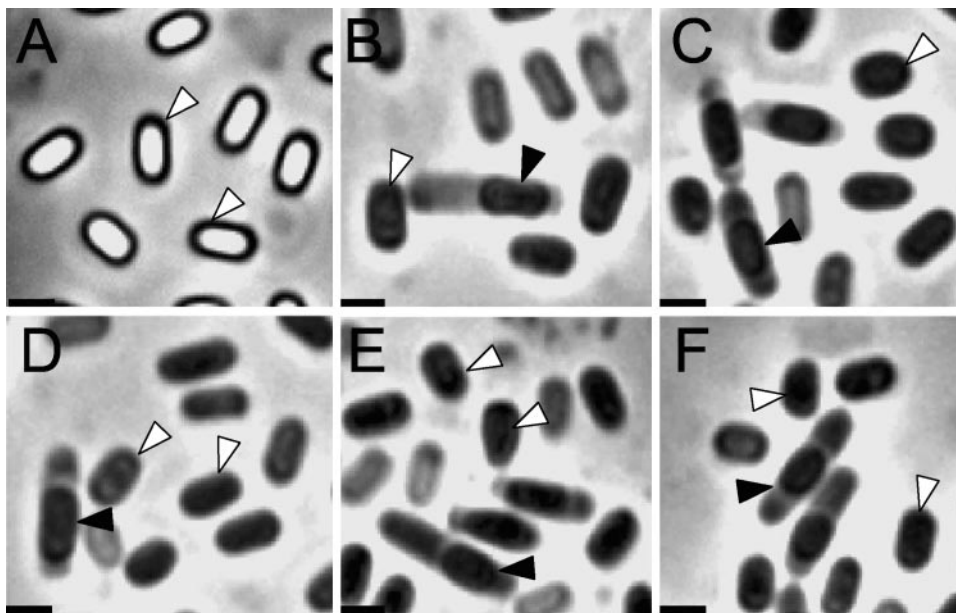
FIG. 6. MurB depletion causes the production of dark-phase spores. The figure depicts spores produced by the wild-type strain MB24 (A) and the *murB* conditional mutant AH3497 (Δ*murB amyE*::P*xylA-murB*) (B through F) in DSM medium in the absence of xylose (A and B) or in the presence of the following xylose concentrations: 0.001% (C), 0.005% (D), 0.01% (E), 0.1% (F). The spores were collected and purified as described in Material and Methods and visualized under phase-contrast microscopy. Open and filled arrowheads point to free spores or to spores still inside the mother cell, respectively. Bars, 2 μm.

morphology, and their growth rate was proportional to the level of *murB* expression.

However, the two strains showed different requirements for MurB for normal growth in liquid medium. The *murB*::*neo* insertional mutant AH1746 required a level of MurB at least three times higher than a congenic wild-type strain for normal growth. The mutant also showed a slight reduction in the level of DivIB, encoded by the downstream *divIB* gene, although not sufficient to perturb normal cell division. However, a second copy of the *divIB* gene permitted normal growth at wild-type levels of MurB, suggesting that DivIB somehow contributes to the normal growth of the *murB* conditional mutant. In agreement with this suggestion, the conditional mutant AH3497, in which the *murB* gene at the *dcw* cluster was deleted in frame, showed normal levels of DivIB and a normal growth rate at wild-type levels of MurB. Separation of *murB* from *divIB* by an integrational plasmid resulted in a strain with reduced levels of DivIB but essentially normal cell division and with a slow growth phenotype (45). The reason for this slow growth phenotype was not clear, but it was not due to a polar effect on genes located downstream of *divIB*, and while a copy of *divIB* in *trans* corrected the slow growth phenotype of the mutant, an extra copy of the *murB* gene aggravated the phenotype (45). This suggested that at least in this strain, a reduction in the levels of DivIB may not be accompanied by a reduction in the levels of MurB. In any case, these observations suggested that *murB* and *divIB* have to be coordinately expressed. Cell division mutants have been reported to show a normal growth rate before cell lysis occurs. However, the function of *divIB* may not be restricted to cell division (45). The suggestion that coordinated expression of *murB* and *divIB* is important for normal growth is in agreement with the presence of the two cistrons in

long polycistronic messages that transverse most of the *dcw* cluster of *B. subtilis* during growth (25) and with the observation that the *spoVE-murG-murB-divIB* unit within the *dcw* cluster appears to be unique to spore formers of the genus *Bacillus*. It could be that in *Bacillus* species, the coordination between synthesis of cell wall precursors and cell division is exerted at least in part at the level of transcription of the *murG-murB-divIB* unit (see also below).

Synthesis of the spore cortex PG is essential for spore heat resistance (3, 17, 18). The spore cortex is formed between the two membranes that surround the prespore at an intermediate stage of development, from precursors that may be produced mainly in the mother cell (3, 17, 18). The activity of the sporulation-specific σ^E factor is confined to the mother cell and is required for transcription of several genes involved in synthesis of the spore cortex PG (e.g., see references 9 and 53). However, synthesis of the spore cortex commences only following the complete engulfment of the prespore by the mother cell, with the concomitant activation of the late mother cell regulator σ^K (3, 17, 18, 43). Activation of σ^K takes place around hour 4 of sporulation, and synthesis of the spore cortex ensues, in parallel with the appearance of bright-phase spores (39). It seems that expression of *murB* during sporulation is required for synthesis of the spore cortex. Increased transcription of the *murG* and *murB* genes is seen during sporulation (15), presumably from the σ^E-dependent promoter of the upstream *spoVE* gene (53), and the levels of MurB increase coincidentally with the period of cortex formation (this work).

Surprisingly, in cells with *murB* absent from the *dcw* cluster, expression of the P*xylA-murB* inducible allele from an ectopic position drastically reduced the frequency of heat-resistant spores and resulted in the accumulation of over 99% dark-

phase spores, a sign of incomplete cortex formation (29, 43). Remarkably, ectopic expression of P*xylA-murB* in cells that kept *murB* at its normal position within the *dcw* cluster did not interfere in any detectable way with the frequency of sporulation of the formation of refractile spores. Hence, displacement of the *murB* gene from its normal location in the *dcw* cluster appears detrimental for cortex formation during sporulation. This is in keeping with the idea that the *spoVE-murG-murB-divIB* unit within the *dcw* region, which is confined to *Bacillus* spore formers (Fig. 1), is of biological importance for this group of organisms. Both *spoVE* and *murG* appear to be involved in the membrane-linked steps of PG synthesis (4, 31). It is tempting to speculate that the clustering of *murG*, *murB*, and *divIB* would contribute to the coordination between synthesis of PG precursors and cell division during the vegetative life cycle and that linkage of at least the *murG-murB* unit to *spoVE* would coordinate PG precursor synthesis to their translocation across the spore membrane for the formation of the spore cortex.

Assembly of the PG molecule involves the sequential addition of L-alanine, D-glutamic acid, diaminopimelic acid, and D-alanyl-D-alanine to the UDP-MurNAc. The observation that the *murB* conditional mutant (AH3497) is more sensitive to D-cycloserine, an inhibitor of the D-alanine racemase (Alr) and of D-alanyl-D-alanine ligase (Ddl), suggests that a reduction in the efficiency of the MurB-catalyzed step of the PG biosynthetic pathway will lead to a rapid depletion of downstream precursors, and as a consequence it will make these cells more sensitive to any antibiotic acting downstream of that step. At suboptimal concentrations of inducer, the increased susceptibility of the mutant to D-cycloserine and to the β-lactamic antibiotics oxacillin and cephalosporin suggests that its cell wall may accumulate tripeptide muropeptides. If so, a further decrease in cross-linking caused by β-lactam antibiotics could compromise the structural stability of the cell wall. That resistance to the β-lactams cephalosporin and oxacillin increases with increased expression of *murB* is reminiscent of the situation with a P*spac-murE* conditional mutant of *S. aureus* (19). At suboptimal levels of inducer, the mutant shows increased susceptibility to oxacillin (19).

In *B. subtilis*, cell wall-active antibiotics induce the extracytoplasmic sigma factors σ^M and σ^W possibly via a chemical or physical signal related to a defect in the structure or composition of the cell wall (5, 52). Significantly, vancomycin, which acts as a potent inducer of *sigW*, and of a large number of σ^W-dependent genes, results in induction of the contiguous *murG*, *murB*, *divIB*, and *ylxW* genes (5). We note that the *murB* conditional mutant is not more susceptible to vancomycin. However, a *sigW* mutant is not significantly affected in its sensitivity to vancomycin (5). It is possible that in *B. subtilis*, increased expression of *murB* in the conditional mutant somehow induces expression of the genes for specific PBPs. However, the pool of soluble PG precursors, or the composition of the cell wall in the *murB* conditional mutant, has not yet been examined, and it is unknown whether σ^W is induced in the P*xylA-murB* mutant.

The *murB* conditional mutant is also more sensitive to fosfomycin, an inhibitor of MurA (16, 49). MurA catalyzes the step immediately upstream of MurB, the production of UDPGlcNAcEP. In vitro experiments have shown that the activity of MurA is inhibited by its reaction product and indicated that this reaction is an important control step in the PG biosynthetic pathway (40). Increased susceptibility to fosfomycin under conditions where MurB levels are low could be caused by accumulation of UDPGlcNAcEP and inhibition of MurA, or simply to the combined effect of inhibition of two consecutive steps in the pathway. In any event, because different steps in the PG biosynthetic pathway appear to be more sensitive to known antibiotics in a way that depends on the expression of *murB*, we suggest that the *murB* conditional mutant could be used as a tool in screening for new antibacterial compounds that act at the level of cell wall biogenesis (13).

ACKNOWLEDGMENTS

REFERENCES

1. **Amabile-Cuevas, C. F., and B. Demple.** 1991. Molecular characterization of the *soxRS* genes of *Escherichia coli*: two genes control a superoxide stress regulon. Nucleic Acids Res. **19:**4479–4484.
2. **Ariza, R. R., S. P. Cohen, N. Bachhawat, S. B. Levy, and B. Demple.** 1994. Repressor mutations in the *marRAB* operon that activate oxidative stress genes and multiple antibiotic resistance in *Escherichia coli*. J. Bacteriol. **176:**143–148.
3. **Buchanan, C. E., A. O. Henriques, and P. J. Piggot.** 1993. Wall metabolism during sporulation, p. 167–186. *In* J.-M. Ghuysen and R. Hakenback (ed.), Bacterial cell wall, vol. 8. Elsevier Science Publishers, New York, N.Y.
4. **Bupp, K., and J. van Heijenoort.** 1993. The final step of peptidoglycan subunit assembly in *Escherichia coli* occurs in the cytoplasm. J. Bacteriol. **175:**1841–1843.
5. **Cao, M., T. Wang, R. Ye, and J. D. Helmann.** 2002. Antibiotics that inhibit cell wall biosynthesis induce expression of the *Bacillus subtilis* sigma(W) and sigma(M) regulons. Mol. Microbiol. **45:**1267–1276.
6. **Carballido-Lopez, R., and J. Errington.** 2003. A dynamic bacterial cytoskeleton. Trends Cell Biol. **13:**577–583.
7. **Cunningham, R. P., S. M. Saporito, S. G. Spitzer, and B. Weiss.** 1986. Endonuclease IV (*nfo*) mutant of *Escherichia coli*. J. Bacteriol. **168:**1120–1127.
8. **Cutting, S. M., and P. B. Vander Horn.** 1990. Genetic analysis, p. 27–74. *In* C. R. Harwood and S. M. Cutting (ed.), Molecular biology methods for *Bacillus*. John Wiley and Sons, Ltd., New York, N.Y.
9. **Daniel, R. A., S. Drake, C. E. Buchanan, R. Scholle, and J. Errington.** 1994. The *Bacillus subtilis spoVD* gene encodes a mother-cell-specific penicillin-binding protein required for spore morphogenesis. J. Mol. Biol. **235:**209–220.
10. **Daniel, R. A., and J. Errington.** 2003. Control of cell morphogenesis in bacteria: two distinct ways to make a rod-shaped cell. Cell **113:**767–776.
11. **Daniel, R. A., E. J. Harry, and J. Errington.** 2000. Role of penicillin-binding protein PBP 2B in assembly and functioning of the division machinery of *Bacillus subtilis*. Mol. Microbiol. **35:**299–311.
12. **Daniel, R. A., A. M. Williams, and J. Errington.** 1996. A complex four-gene operon containing essential cell division gene *pbpB* in *Bacillus subtilis*. J. Bacteriol. **178:**2343–2350.
13. **DeVito, J. A., J. A. Mills, V. G. Liu, A. Agarwal, C. F. Sizemore, Z. Yao, D. M. Stoughton, M. G. Cappiello, M. D. Barbosa, L. A. Foster, and D. L. Pompliano.** 2002. An array of target-specific screening strains for antibacterial discovery. Nat. Biotechnol. **20:**478–483.
14. **Eichenberger, P., M. Fujita, S. T. Jensen, E. M. Conlon, D. Z. Rudner, S. T. Wang, C. Ferguson, K. Haga, T. Sato, J. S. Liu, and R. Losick.** 2004. The program of gene transcription for a single differentiating cell type during sporulation in *Bacillus subtilis*. PLoS Biol. **2:**e328.
15. **Eichenberger, P., S. T. Jensen, E. M. Conlon, C. van Ooij, J. Silvaggi, J. E. Gonzalez-Pastor, M. Fujita, S. Ben-Yehuda, P. Stragier, J. S. Liu, and R. Losick.** 2003. The sigmaE regulon and the identification of additional sporulation genes in *Bacillus subtilis*. J. Mol. Biol. **327:**945–972.
16. **El Zoeiby, A., F. Sanschagrin, and R. C. Levesque.** 2003. Structure and function of the Mur enzymes: development of novel inhibitors. Mol. Microbiol. **47:**1–12.
17. **Errington, J.** 2003. Regulation of endospore formation in *Bacillus subtilis*. Nat. Rev. Microbiol. **1:**117–126.

18. **Foster, S. J., and D. L. Popham.** 2002. Structure and synthesis of cell wall, spore cortex, teichoic acids, S-layers, and capsules, p. 21–42. *In* A. L. Sonenshein, J. A. Hoch, and R. Losick (ed.), *Bacillus subtilis* and its closest relatives: from genes to cells. American Society for Microbiology, Washington, D.C.

19. **Gardete, S., A. M. Ludovice, R. G. Sobral, S. R. Filipe, H. de Lencastre, and A. Tomasz.** 2004. Role of *murE* in the expression of beta-lactam antibiotic resistance in *Staphylococcus aureus*. J. Bacteriol. **186:**1705–1713.

20. **Gholamhoseinian, A., Z. Shen, J. J. Wu, and P. Piggot.** 1992. Regulation of transcription of the cell division gene *ftsA* during sporulation of *Bacillus subtilis*. J. Bacteriol. **174:**4647–4656.

21. **Gonzy-Treboul, G., C. Karmazyn-Campelli, and P. Stragier.** 1992. Developmental regulation of transcription of the *Bacillus subtilis ftsAZ* operon. J. Mol. Biol. **224:**967–979.

22. **Greenberg, J. T., J. H. Chou, P. A. Monach, and B. Demple.** 1991. Activation of oxidative stress genes by mutations at the *soxQ/cfxB/marA* locus of *Escherichia coli*. J. Bacteriol. **173:**4433–4439.

23. **Greenberg, J. T., P. Monach, J. H. Chou, P. D. Josephy, and B. Demple.** 1990. Positive control of a global antioxidant defense regulon activated by superoxide-generating agents in *Escherichia coli*. Proc. Natl. Acad. Sci. USA **87:**6181–6185.

24. **Guerout-Fleury, A. M., N. Frandsen, and P. Stragier.** 1996. Plasmids for ectopic integration in *Bacillus subtilis*. Gene **180:**57–61.

25. **Harry, E. J., S. L. Rowland, M. S. Malo, and R. G. Wake.** 1994. Expression of *divIB* of *Bacillus subtilis* during vegetative growth. J. Bacteriol. **176:**1172–1179.

26. **Henriques, A. O., B. W. Beall, and C. P. Moran, Jr.** 1997. CotM of *Bacillus subtilis*, a member of the alpha-crystallin family of stress proteins, is induced during development and participates in spore outer coat formation. J. Bacteriol. **179:**1887–1897.

27. **Henriques, A. O., B. W. Beall, K. Roland, and C. P. Moran, Jr.** 1995. Characterization of *cotJ*, a σ^E-controlled operon affecting the polypeptide composition of the coat of *Bacillus subtilis* spores. J. Bacteriol. **177:**3394–3406.

28. **Henriques, A. O., E. M. Bryan, B. W. Beall, and C. P. Moran, Jr.** 1997. *cse15*, *cse60*, and *csk22* are new members of mother-cell-specific sporulation regulons in *Bacillus subtilis*. J. Bacteriol. **179:**389–398.

29. **Henriques, A. O., H. de Lencastre, and P. J. Piggot.** 1992. A *Bacillus subtilis* morphogene cluster that includes *spoVE* is homologous to the *mra* region of *Escherichia coli*. Biochimie **74:**735–748.

30. **Henriques, A. O., P. Glaser, P. J. Piggot, and C. P. Moran, Jr.** 1998. Control of cell shape and elongation by the *rodA* gene in *Bacillus subtilis*. Mol. Microbiol. **28:**235–247.

31. **Ikeda, M., T. Sato, M. Wachi, H. K. Jung, F. Ishino, Y. Kobayashi, and M. Matsuhashi.** 1989. Structural similarity among *Escherichia coli* FtsW and RodA proteins and *Bacillus subtilis* SpoVE protein, which function in cell division, cell elongation, and spore formation, respectively. J. Bacteriol. **171:**6375–6378.

32. **Itaya, M., K. Kondo, and T. Tanaka.** 1989. A neomycin resistance gene cassette selectable in a single copy state in the *Bacillus subtilis* chromosome. Nucleic Acids Res. **17:**4410.

33. **Jones, L. J., R. Carballido-Lopez, and J. Errington.** 2001. Control of cell shape in bacteria: helical, actin-like filaments in *Bacillus subtilis*. Cell **104:**913–922.

34. **Kanehisa, M.** 1997. Linking databases and organisms: GenomeNet resources in Japan. Trends Biochem. Sci. **22:**442–444.

35. **Kanehisa, M., S. Goto, S. Kawashima, and A. Nakaya.** 2002. The KEGG databases at GenomeNet. Nucleic Acids Res. **30:**42–46.

36. **Karow, M. L., and P. J. Piggot.** 1995. Construction of *gusA* transcriptional fusion vectors for *Bacillus subtilis* and their utilization for studies of spore formation. Gene **163:**69–74.

37. **Marty, N., L. Agueda, V. Carratala, and G. Chabanon.** 1994. Evaluation of the Spiral method to determine the MIC of various antibiotics. Pathol. Biol. (Paris) **42:**448–453.

38. **Matsuo, M., K. Kurokawa, S. Nishida, Y. Li, H. Takimura, C. Kaito, N. Fukuhara, H. Maki, K. Miura, K. Murakami, and K. Sekimizu.** 2003. Isolation and mutation site determination of the temperature-sensitive *murB* mutants of *Staphylococcus aureus*. FEMS Microbiol. Lett. **222:**107–113.

39. **Meador-Parton, J., and D. L. Popham.** 2000. Structural analysis of *Bacillus subtilis* spore peptidoglycan during sporulation. J. Bacteriol. **182:**4491–4499.

40. **Mengin-Lecreulx, D., B. Flouret, and J. van Heijenoort.** 1983. Pool levels of UDP *N*-acetylglucosamine and UDP *N*-acetylglucosamine-enolpyruvate in *Escherichia coli* and correlation with peptidoglycan synthesis. J. Bacteriol. **154:**1284–1290.

41. **Miyakawa, T., H. Matsuzawa, M. Matsuhashi, and Y. Sugino.** 1972. Cell wall peptidoglycan mutants of *Escherichia coli* K-12: existence of two clusters of genes, *mra* and *mrb*, for cell wall peptidoglycan biosynthesis. J. Bacteriol. **112:**950–958.

42. **Miyao, A., G. Theeragool, M. Takeuchi, and Y. Kobayashi.** 1993. *Bacillus subtilis spoVE* gene is transcribed by σ^E-associated RNA polymerase. J. Bacteriol. **175:**4081–4086.

43. **Piggot, P. J., and J. G. Coote.** 1976. Genetic aspects of bacterial endospore formation. Bacteriol. Rev. **40:**908–962.

44. **Pucci, M. J., L. F. Discotto, and T. J. Dougherty.** 1992. Cloning and identification of the *Escherichia coli murB* DNA sequence, which encodes UDP-*N*-acetylenolpyruvoylglucosamine reductase. J. Bacteriol. **174:**1690–1693.

45. **Real, G., S. Autret, E. J. Harry, J. Errington, and A. O. Henriques.** 2005. Cell division protein DivIB influences the Spo0J/Soj system of chromosome segregation in *Bacillus subtilis*. Mol. Microbiol. **55:**349–367.

46. **Rowland, S. L., J. Errington, and R. G. Wake.** 1995. The *Bacillus subtilis* cell-division 135-137 degree region contains an essential orf with significant similarity to *murB* and a dispensable sbp gene. Gene **164:**113–116.

47. **Serrano, M., R. Zilhao, E. Ricca, A. J. Ozin, C. P. Moran, Jr., and A. O. Henriques.** 1999. A *Bacillus subtilis* secreted protein with a role in endospore coat assembly and function. J. Bacteriol. **181:**3632–3643.

48. **Seyler, R. W., Jr., A. O. Henriques, A. J. Ozin, and C. P. Moran, Jr.** 1997. Assembly and interactions of *cotJ*-encoded proteins, constituents of the inner layers of the *Bacillus subtilis* spore coat. Mol. Microbiol. **25:**955–966.

49. **Silver, L. L.** 2003. Novel inhibitors of bacterial cell wall synthesis. Curr. Opin. Microbiol. **6:**431–438.

50. **Sterlini, J. M., and J. Mandelstam.** 1969. Commitment to sporulation in *Bacillus subtilis* and its relationship to development of actinomycin resistance. Biochem. J. **113:**29–37.

51. **Tamames, J., M. Gonzalez-Moreno, J. Mingorance, A. Valencia, and M. Vicente.** 2001. Bringing gene order into bacterial shape. Trends Genet. **17:**124–126.

52. **Thackray, P. D., and A. Moir.** 2003. SigM, an extracytoplasmic function sigma factor of *Bacillus subtilis*, is activated in response to cell wall antibiotics, ethanol, heat, acid, and superoxide stress. J. Bacteriol. **185:**3491–3498.

53. **Theeragool, G., A. Miyao, K. Yamada, T. Sato, and Y. Kobayashi.** 1993. In vivo expression of the *Bacillus subtilis spoVE* gene. J. Bacteriol. **175:**4071–4080.

54. **van den Ent, F., L. A. Amos, and J. Lowe.** 2001. Prokaryotic origin of the actin cytoskeleton. Nature **413:**39–44.

55. **van Heijenoort, J.** 1996. Murein synthesis, p. 1025–1034. *In* F. C. Neidhardt, R. Curtis III, J. L. Ingraham, E. C. C. Lin, K. B. Low, B. Magasanik, W. S. Reznikoff, M. Riley, M. Schaecter, and H. E. Umbarger (ed.), *Escherichia coli* and *Salmonella*: cellular and molecular biology, vol. 1. American Society for Microbiology, Washington, D.C.

56. **Varley, A. W., and G. C. Stewart.** 1992. The *divIVB* region of the *Bacillus subtilis* chromosome encodes homologs of *Escherichia coli* septum placement (*minCD*) and cell shape (*mreBCD*) determinants. J. Bacteriol. **174:**6729–6742.

57. **Wei, Y., T. Havasy, D. C. McPherson, and D. L. Popham.** 2003. Rod shape determination by the *Bacillus subtilis* class B penicillin-binding proteins encoded by *pbpA* and *pbpH*. J. Bacteriol. **185:**4717–4726.

58. **Yanouri, A., R. A. Daniel, J. Errington, and C. E. Buchanan.** 1993. Cloning and sequencing of the cell division gene *pbpB*, which encodes penicillin-binding protein 2B in *Bacillus subtilis*. J. Bacteriol. **175:**7604–7616.

59. **Zilhao, R., G. Naclerio, A. O. Henriques, L. Baccigalupi, C. P. Moran, Jr., and E. Ricca.** 1999. Assembly requirements and role of CotH during spore coat formation in *Bacillus subtilis*. J. Bacteriol. **181:**2631–2633.